Applied and Environmental Microbiology, Oct. 2010, p. 6910–6919 Vol. 76, No. 20
0099-2240/10/$12.00 doi:10.1128/AEM.01375-10

Link between Phosphate Starvation and Glycogen Metabolism in *Corynebacterium glutamicum*, Revealed by Metabolomics▽†

Han Min Woo,[1] Stephan Noack,[2] Gerd M. Seibold,[3,5] Sabine Willbold,[4] Bernhard J. Eikmanns,[3] and Michael Bott[1]*

Institute of Biotechnology 1, Forschungszentrum Jülich, D-52425 Jülich, Germany[1]; Institute of Biotechnology 2, Forschungszentrum Jülich, D-52425 Jülich, Germany[2]; Institute of Microbiology and Biotechnology, Ulm University, D-89081 Ulm, Germany[3]; Central Division of Analytical Chemistry, Forschungszentrum Jülich, D-52425 Jülich, Germany[4]; and Institute of Biochemistry, University of Cologne, D-50674 Cologne, Germany[5]

Received 9 June 2010/Accepted 14 August 2010

In this study, we analyzed the influence of phosphate (P_i) limitation on the metabolism of *Corynebacterium glutamicum*. Metabolite analysis by gas chromatography–time-of-flight (GC-TOF) mass spectrometry of cells cultivated in glucose minimal medium revealed a greatly increased maltose level under P_i limitation. As maltose formation could be linked to glycogen metabolism, the cellular glycogen content was determined. Unlike in cells grown under P_i excess, the glycogen level in P_i-limited cells remained high in the stationary phase. Surprisingly, even acetate-grown cells, which do not form glycogen under P_i excess, did so under P_i limitation and also retained it in stationary phase. Expression of *pgm* and *glgC*, encoding the first two enzymes of glycogen synthesis, phosphoglucomutase and ADP-glucose pyrophosphorylase, was found to be increased 6- and 3-fold under P_i limitation, respectively. Increased glycogen synthesis together with a decreased glycogen degradation might be responsible for the altered glycogen metabolism. Independent from these experimental results, flux balance analysis suggested that an increased carbon flux to glycogen is a solution for *C. glutamicum* to adapt carbon metabolism to limited P_i concentrations.

Phosphorus is an essential nutrient for all cells and is required for, e.g., the biosynthesis of nucleotides, NAD(P)H, DNA, and RNA but also for the regulation of protein activity by phosphorylation of histidine, aspartate, serine, threonine, or tyrosine residues. A common phosphorus source is inorganic phosphate (P_i), and cells have developed mechanisms for the acquisition, assimilation, and storage of P_i. When P_i becomes limiting, many bacteria induce the synthesis of proteins that enable them to capture the residual P_i resources more efficiently and to make alternative phosphorus sources accessible. The corresponding genes are collectively named P_i starvation-inducible genes, or *psi* genes. The P_i starvation response, and in particular its regulation, has been most carefully studied in *Escherichia coli* (45) and *Bacillus subtilis* (14).

We recently started to characterize the P_i starvation response in *Corynebacterium glutamicum*, a Gram-positive soil bacterium used industrially for the production of more than two millions tons of amino acids per year, mainly L-glutamate and L-lysine (12). An overview of the biology, genetics, physiology, and application of *C. glutamicum* can be found in two recent monographs (3, 6). Phosphorus constitutes 1.5% to 2.1% of the cell dry weight of *C. glutamicum* (24), part of which can be present as polyphosphate (22, 29). Several of the enzymes involved in polyphosphate metabolism have been characterized recently, such as a class II polyphosphate kinase (28), the exopolyphosphatases Ppx1 and Ppx2 (26), a polyphosphate/ATP-dependent glucokinase (25), and a polyphosphate/ATP-dependent NAD^+ kinase (27). The P_i starvation stimulon of *C. glutamicum* was determined using whole-genome DNA microarrays (15). Comparison of the mRNA profiles before and at different times after a shift from P_i excess to P_i starvation led to the identification of a group of genes that are presumably required to cope with limited P_i supply. This group includes the following: the *pstSCAB* operon, encoding an ABC transporter for high-affinity P_i uptake; the *ugpAEBC* operon, encoding an ABC transporter for uptake of glycerol 3-phosphate; *glpQ1*, encoding a glycerophosphoryl diester phosphodiesterase; *ushA*, encoding a secreted enzyme with UDP-sugar hydrolase and 5′-nucleotidase activities (33); *nucH*, encoding a putative secreted nuclease which possibly plays a role in liberating P_i from extracellular nucleic acids; *phoC* (NCgl2959/*cg3393*), which may encode a cell wall-associated phosphatase (46); *phoH1*, encoding an ATPase of unknown function; and the *pctABCD* operon, encoding an ABC transport system which might be involved in the uptake of a yet-unknown phosphorus-containing compound (15). *C. glutamicum* lacks homologs of genes for phosphonate degradation, as well as the capability to utilize phosphonates as P sources (15).

In most bacteria analyzed in this respect, the P_i starvation response is controlled by two-component signal transduction systems, e.g., the PhoBR system in *E. coli* (13) and the PhoPR system in *B. subtilis* (14). Our previous studies revealed that in *C. glutamicum*, a two-component system composed of the sensor kinase PhoS and the response regulator PhoR is involved in the activation of phosphate starvation-inducible genes (21). Studies with purified proteins showed that phosphorylation by

* Corresponding author. Mailing address: Institute of Biotechnology 1, Forschungszentrum Jülich, D-52425 Jülich, Germany. Phone: 49 2461 613294. Fax: 49 2461 612710. E-mail: m.bott@fz-juelich.de.

† Supplemental material for this article may be found at http://aem.asm.org/.

▽ Published ahead of print on 27 August 2010.

TABLE 1. Strains and plasmids used in this study

Strain or plasmid	Relevant characteristics	Source or reference
Strains		
E. coli DH5α	F^- *thi-1 endA1 hsdR17*(r^- m^-) *supE44* Δ*lacU169* (ϕ80*lacZ*ΔM15) *recA1 gyrA96 relA1*	Invitrogen
C. glutamicum ATCC 13032	Biotin-auxotrophic wild-type strain	19
C. glutamicum Δ*sugR*	ATCC 13032 derivative with an in-frame deletion of *sugR*	9
C. glutamicum IMC	ATCC 13032 derivative with a disruption of *glgC*	36
Plasmids		
pET2	Kan^r; promoter-probe vector for *C. glutamicum*	44
pET2-*pgm*	Kan^r; pET2 with a 423-bp fragment covering the *pgm* promoter (−413 to +10 with respect to the proposed translational start site)	This study
pET2-*glgC*	Kan^r; pET2 with a 406-bp fragment covering the *glgC* promoter (−402 to +4 with respect to the proposed translational start site)	This study

PhoS increased the DNA-binding affinity of PhoR, which bound to many of the P_i starvation-inducible genes, but with different affinities (34).

The study reported here was initiated by the question how the metabolism of *C. glutamicum* responds to P_i limitation. Our results reveal a link between P_i limitation and glycogen metabolism, which was also used for metabolic simulations based on a genome-wide metabolic model.

MATERIALS AND METHODS

Strains and cultivation. The strains and plasmids used in this study are listed in Table 1. The wild-type *C. glutamicum* strain ATCC 13032, its *glgC* disruption mutant (36), and its Δ*sugR* mutant (9) were precultivated aerobically at 30°C in baffled 500-ml shake flasks on a rotary shaker at 120 rpm using CGIII complex medium (10 g peptone, 10 g yeast extract, and 25 g NaCl per liter) supplemented with 222 mM glucose. After cells had been washed with 0.9% (wt/vol) NaCl, they were transferred to defined CGXII minimal medium (18) supplemented with protocatechuic acid (30 mg/liter) as an iron chelator and either 222 mM glucose or 300 mM potassium acetate as a carbon source. For the analysis of the response of *C. glutamicum* to P_i limitation at the metabolite level, the cells were precultivated twice in CGXII glucose medium with 0.13 mM P_i, and after being washed, they were inoculated into CGXII glucose medium under different P_i conditions (13 mM, 0.65 mM, 0.26 mM, and 0.13 mM). P_i was added as KH_2PO_4 and K_2HPO_4. Samples for metabolite analysis were taken after 8, 12, and 24 h cultivation. For *in vivo* ^{13}C labeling of the metabolites, cells were grown in CGXII medium containing 222 mM uniformly ^{13}C-labeled glucose (Cambridge Isotope Laboratory, Andover, MA) as the sole carbon source under the conditions described above, including two precultivations with ^{13}C-labeled glucose.

Extraction of metabolites and sample preparation for metabolite profiling. One-milliliter samples of triplicate cultures with known optical densities at 600 nm (OD_{600}) were added to 2-ml Eppendorf tubes containing 500 mg of silicon oil (δ = 1.05 g/cm^3) and 300 μl 20% (vol/vol) perchloric acid ($HClO_4$, δ = 1.18 g/cm^3). The tubes were centrifuged immediately at 13,000 rpm for 30 s in order to separate the cells from the culture supernatant and to inactivate metabolism by the acid treatment. After careful removal of the supernatant, the samples were mixed and neutralized with 185 μl of 6 N potassium hydroxide. The pH was controlled by the indicator bromthymol blue, which is green at pH 7. Aliquots of the polar phase, corresponding to 5.0 mg cells (dry weight) [an OD_{600} of 1 corresponds to 0.25 mg cells (dry weight) per ml (16)] were lyophilized for at least 2 days. Subsequently, the dried cell extracts were treated for 90 min at 35°C with 50 μl methoxyamine hydrochloride in pyridine (20 mg/ml) and subsequently trimethylsilated with 80 μl *N*-methyl-*N*-(trimethylsilyl)trifluoroacetamide (MSTFA) for 4 h at 35°C to derivatize the metabolites for gas chromatography–time-of-flight (GC-TOF) mass spectrometry (MS) analysis.

Metabolite pattern analysis. Metabolite pattern analysis was used as an initial approach to determine whether the metabolite patterns of cells differ depending on P_i availability. In a first series of experiments, GC-TOF MS data sets were obtained from cells cultured for 24 h in CGXII glucose medium with different P_i concentrations (13 mM, 0.65 mM, 0.25 mM, and 0.13 mM P_i). In a second series, GC-TOF MS data sets were obtained from three time points (8 h, 12 h, and 24 h) of cultures grown in CGXII glucose medium under either P_i excess (13 mM) or P_i starvation (0.13 mM). To perform metabolite pattern analysis, for each sample a data set containing 2,517 mass fragments (whose chemical identities were unknown) differing in either mass or retention time and identified in all analyzed samples by MarkerLynx software was exported to SIMCA-P+ software (Umetrics AB, Umeå, Sweden). These datasets were analyzed by partial least-squares discriminant analysis (PLS-DA) (47).

GC-(EI/CI)-TOF MS. The derivatized metabolite samples prepared as described above were analyzed by GC-TOF MS using both the electron ionization (EI+) mode and chemical ionization (CI+) mode. The GC-TOF MS system was composed of an Agilent gas chromatograph 6890N (Agilent, Santa Clara, CA) equipped with a Gerstel MPS2 multipurpose sampler (Gerstel, Mülheim, Germany) and a GCT Premier benchtop orthogonal acceleration time-of-flight mass spectrometer (Waters, Milford, MA). The system was operated using MassLynx software (version 4.1; Waters). GC was performed using a 30-m by 0.25-μm DB-5MS column (J&W Scientific, Folsom, CA) with a constant flow rate of 1 ml/min of helium as the carrier gas. After the needle of the injector syringe had been washed with hexane and methanol, 1 μl of sample was injected with a split ratio of 2:1 at 280°C to a glass liner (4-mm inner diameter) filled with glass wool. For GC separation, the oven temperature stayed initially for 2 min at 85°C and then increased to 320°C by 15°C/min, where it was held for 5 min. Transfer of the samples from the GC to the mass spectrometer was performed at 150°C.

Evaporated chemicals were ionized by either the EI or CI method. For EI+, the ionization energy was tuned at 70 eV according to the operation manual using heptacosafluorotributylamine [$(C_4F_9)_3N$] as an internal reference. For positive chemical ionization (CI+), isobutene (0.7 bar, 10^{-5} mbar in the source) as a reagent gas generated ionized $[MH]^+$, $[M + C_4H_9]^+$, and $[M + C_3H_3]^+$ quasi-molecules at an electron energy of 50 eV. Tuning for the CI+ mode was performed according to the operation manual using 2,4,6-tri(trifluoromethyl)-1,3,5-triazine as an internal reference. Mass ions were detected with the scan time set to 0.9 s and the interscan set to 0.1 s in the centroid mode using lock mass at 218.9856 *m/z*. Mass fragment patterns were analyzed to identify metabolites using NIST MS search with several public libraries and a homemade library.

Metabolite identification by GC-(EI/CI)-TOF MS based on the use of naturally and uniformly ^{13}C-labeled metabolites. GC-MS has been widely used to analyze volatile chemicals and derivatized chemicals because of high sensitivities and the availability of standard mass fragment libraries. In general, the identification process in GC-MS depends on the matching score of mass fragment patterns between analytes and standards with the same retention time or the index number only when mass fragment libraries of standards are available. However, a number of peaks with low matching scores (below 700) show ambiguous metabolite identification or remain unknown because of the incompleteness of biological metabolite databases and the possibility of undesired reactions by using highly reactive derivatization chemicals. Therefore, in this study an additional procedure was used to identify "real" metabolites among possible chemicals from derivatized cell extracts. The method is based on the comparison of uniformly ^{13}C-labeled metabolites with naturally labeled metabolites, which were measured separately. By combining all information obtained from the extracts of the cultures grown with either unlabeled or ^{13}C-labeled glucose using the EI/CI ionization methods, metabolites were identified by several criteria as outlined in Fig. S1 in the supplemental material. In the case of mass fragments that still remained unknown after this protocol, identification was attempted based on the exact mass measurement using a Matlab script, which searches possible chemical compositions online in publicly available chemical databases

(Pubchem and KEGG compound DB). The details of this procedure are described in the supplemental material.

Analysis of phosphorus-containing metabolites using ^{31}P *in vivo* NMR spectroscopy. ^{31}P nuclear magnetic resonance (NMR) analysis was performed essentially as described previously (28). Cultures were harvested in the mid-exponential growth phase (8 h) and in the stationary phase (24 h). One gram (wet weight) of cell pellet was suspended in 4 ml absolute ethanol, mixed for 1 min, and centrifuged for 10 min at 4,400 × *g* and 4°C. The supernatant was discarded, and the pellet was resuspended in a mixture of 1.1 ml fresh bi-distilled water, 0.3 ml 1 M EDTA (pH 8.2), and 0.6 ml D_2O. Seven hundred microliters of a 2-ml cell suspension was transferred into a 5-mm NMR tube and analyzed. During preparation, all samples were kept on ice or were kept frozen until further use.

The ^{31}P-NMR spectra were measured at 5°C on a Varian Inova 400 MHz spectrometer. An amount of D_2O sufficient to obtain a stable lock signal was added to each sample prior to measurement. The following parameters were used: frequency, 161,985 MHz; excitation pulse width, 9.25 μs; pulse repetition delay, 1 s; and spectral width, 18.35 kHz. Routine spectra were acquired with 4,096 scans. Chemical shifts were referenced to 85% orthophosphoric acid (0 ppm). Standards of P_i and polyphosphate ("P68" with polymerization from 10 to 40; BK Giulini Chemie, Ladenburg, Germany) were prepared with final concentrations of 10 mM, in terms of P_i (29). Signals were integrated with the MestRe Nova software (Mestrelab Research, Santiago, Spain) to quantify total intracellular P_i and phosphorus-containing metabolites, e.g., phosphomonoesters such as sugar phosphates, NDP-glucose, or polyphosphate.

Measurement of intracellular glycogen contents. The glycogen contents of *C. glutamicum* were determined by the enzymatic method as described previously (31, 35). A culture volume corresponding to 12.5 mg cells (dry weight) [an OD_{600} of 1 corresponds to 0.25 mg/ml cells (dry weight) (16)] was centrifuged, and the cells were washed twice with TN buffer (50 mM Tris-HCl [pH 6.3], 50 mM NaCl). After centrifugation, the cell pellet was resuspended in 1 ml of 40 mM potassium acetate buffer (pH 4.2) and transferred to 2-ml safe-lock Eppendorf tubes filled with 250 mg zirconia/silica beads (0.1 mm diameter). After inactivation of cell-bound glycosidic activity by incubation at 99°C for 5 min, the cells were disrupted by two 30-s rounds of bead beating at 4,500 rpm using a Silamat S5 (Ivoclar Vivadent, Ellwangen, Germany). The cell debris and glass beads were separated from the supernatant by centrifugation (13,000 × *g*, 20 min), and the supernatant was collected and stored at −20°C until use. Each sample was divided into two 100-μl aliquots (labeled sample A and sample B). Two microliters of amyloglucosidase (10 mg/ml; Roche Diagnostics, Mannheim, Germany) was added to sample A to degrade glycogen to free glucose, whereas sample B served as a reference. Both samples were incubated for 2 h at 57°C with shaking at 850 rpm. Subsequently, the glucose concentration in the two samples was determined using a coupled enzymatic assay with hexokinase and glucose 6-phosphate dehydrogenase (Roche Diagnostics, Mannheim, Germany) by measuring the NADH formed at 340 nm. Finally, the glycogen content was calculated in mg per g of cells (dry weight) after subtraction of the glucose concentration of the reference sample B from that of the test sample A.

Construction of transcriptional fusions and chloramphenicol acetyltransferase (CAT) assays. For CAT assays, DNA fragments covering the promoter regions of the *pgm* and *glgC* genes were amplified and cloned into the corynebacterial promoter-probe vector pET2 (44), resulting in the plasmids pET2-*pgm* and pET2-*glgC*, respectively (Table 1). The cloned fragments were controlled by DNA sequence analysis. The plasmids were introduced into wild-type *C. glutamicum*, and the transformed strains were cultivated as outlined above. The CAT assays were performed as described previously (9).

Constraint-based analysis using a genome-scale model of *C. glutamicum*. Flux balance analysis (FBA) was performed using a slightly modified version of the genome-scale model of *C. glutamicum* ATCC 13032 (20) consisting of 446 metabolic reactions and 411 metabolites. The following additional reactions for glycogen formation and degradation were considered as described in reference 36: for GlgC, G1P + ATP → ADP-GLC + PP_i; for GlgA, ADP-GLC → GLGN + ADP; and for GlgP and MalP, GLGN + P_i → G1P. For this network, steady-state flux distributions were calculated by FBA using linear programming-based optimization of growth as cellular objective function. In order to obtain feasible phenotypic spaces related to the experimentally observed P_i starvation response of *C. glutamicum*, the flux cone was constrained to different combinations of uptakes rates for P_i and glucose or acetate as carbon sources (32). In addition, only by-products that were observed during the growth experiments were allowed to be formed. For these fluxes, upper bounds were defined that were estimated from the quantitative experimental data generated by high-pressure liquid chromatography (HPLC) analysis. This refers to lactate, acetate, fumarate, and malate for glucose-grown cells, whose formation rates were estimated to be 0.10, 0.02, 0.01, and 0.01 mmol g of cells (dry weight)$^{-1}$ h^{-1}, respectively. All simulations were performed under MATLAB (R2008b; Mathworks) using the COBRA toolbox with the LP solver GLPK (1).

RESULTS

Influence of different P_i concentrations on the metabolite pattern of *C. glutamicum* cells. In order to determine the consequences of P_i limitation at the metabolite level, metabolome analysis was performed by GC-TOF mass spectrometry (GC-TOF MS) and the resulting data were analyzed by PLS-DA as a tool for multivariate data analysis (23). For this purpose, *Corynebacterium glutamicum* wild type was cultivated at four different initial P_i concentrations (13 mM, 0.65 mM, 0.26 mM, and 0.13 mM) in CGXII glucose minimal medium. The highest concentration is the one regularly used in this medium. Growth of the cells was comparable to that reported previously (15) and is shown in Fig. 1A. The cells were collected after 24 h of cultivation, intracellular metabolites were extracted and analyzed by GC-TOF MS, and PLS-DA was performed with the data from 2,517 mass fragments that were identified. The resulting score plot for metabolite pattern analysis is shown in Fig. 1B. It is obvious that the samples obtained from cells grown with 13 mM, 0.65 mM, and 0.13 mM P_i formed three distinct groups, whereas the samples obtained from cells grown with 0.26 mM P_i formed two subgroups, one being located close to the 0.65 mM group and the other next to the 0.13 mM group. This analysis was based on mass fragment patterns only rather than on a set of identified metabolites, and it clearly indicated that different P_i concentrations in the medium affect the metabolite composition within the cells. For the following experiments, P_i was used at 13 mM for P_i excess conditions and 0.13 mM for P_i-limiting conditions.

In a second series of experiments, *C. glutamicum* was grown in glucose medium either with 13 mM P_i or with 0.13 mM P_i and samples for GC-TOF MS were taken after 8 h, 12 h, and 24 h of cultivation. The experiment was performed in triplicate starting with independent cultures and resulted in 18 metabolite data sets that again were analyzed by PLS-DA. As shown in Fig. 1C, except for two data sets (P_i excess culture after 8 h and P_i-limited culture after 12 h) which overlapped, all other data sets formed distinct groups on the score plot. For further analysis, cells cultivated for 24 h were used.

Semiquantitative comparison of metabolites in cells cultivated under P_i excess or P_i starvation. In order to get more detailed insights into the changes at the metabolite level that occur under P_i limitation, a semiquantitative comparison was performed in which the metabolomes of cells grown in triplicate for 24 h under P_i excess (13 mM) or P_i starvation (0.13 mM) were analyzed by GC-TOF MS using both electron ionization and chemical ionization. For this purpose, one culture was grown with naturally labeled glucose, whereas the other one was grown with $^{13}C_6$-glucose. The availability of uniformly ^{13}C-labeled metabolites was useful for the identification of the mass fragments detected by GC MS (see the supplemental material).

Table 2 lists metabolites that could be unequivocally identified in the samples. The pool of cytoplasmic P_i was calculated to be 3-fold lower in the P_i-limited cells, which is in contrast to the 100-fold-lower P_i concentration in the medium at the start of the cultivation. It reflects the capability of the cells to main-

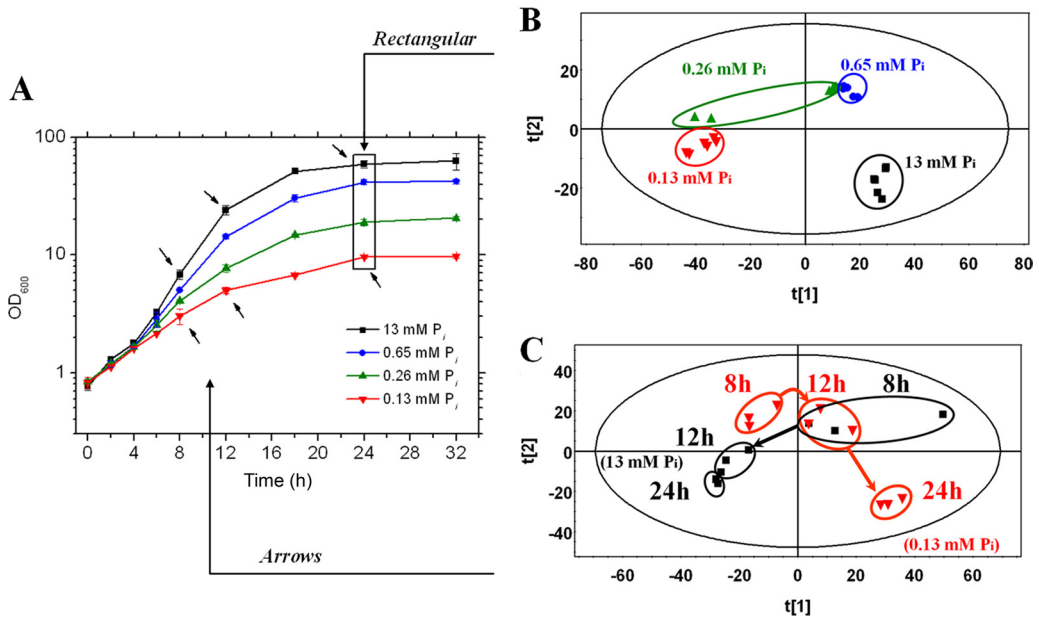

FIG. 1. Influence of growth with different P_i concentrations on the metabolome of *C. glutamicum*. (A) Growth of *C. glutamicum* ATCC 13032 in CGXII minimal medium with 222 mM glucose and different concentration of P_i. Cells were precultured twice in CGXII glucose medium with 0.13 mM potassium P_i and then transferred to CGXII medium containing 0.13 mM, 0.26 mM, 0.65 mM, or 13 mM inorganic P_i. The experiment was performed in triplicate, and mean values and standard deviations are shown. After 24 h, samples of all cultures were taken and used for metabolite analysis by GC-TOF MS. The 2,517 mass fragments detected in all samples were used for PLS-DA, representing one symbol of the score plots. (B) PLS-DA score plot of the metabolome samples taken after 24 h of growth with different P_i concentrations. t[1] and t[2] represent vectors for the most significant components of the matrix *x* of mass ion abundances. The plot shows a directionality of the metabolite pattern from P_i excess to limitation. (C) PLS-DA score plot of the samples taken after 8, 12, and 24 h from cultures grown in CGXII glucose medium with either 13 mM P_i or 0.13 mM P_i.

tain a comparably high cytoplasmic P_i concentration when the external P_i is limiting, due to the activation of the P_i starvation response. The lower level of lactic acid in P_i-limited cells corresponds to the fact that P_i-limited cultures did not produce L-lactate, whereas the P_i excess cultures did (Fig. 2A). Lactate excretion during growth on glucose is usually caused by oxygen limitation, and because of the much lower glucose consumption rate of the P_i-limited cells, no oxygen limitation occurred.

TABLE 2. Relative ratio of identified metabolites during growth of *C. glutamicum* under P_i limitation and P_i excess

Name	Derivatization(s)	Monoisotopic mass (Da)	RT (min)[a]	RI[b]	Area[c] (P_i limitation/P_i excess)	Area ratio (P_i limit./ P_i excess)	*P* value[d]
Lactic acid	2TMS[e]	234.1108	5.48	1,033	7,337 ± 295/384,667 ± 48,336	0.02	0.005
Glycolic acid	2TMS	220.0951	5.67	1,041	15,300 ± 2,307/5,483 ± 361	2.79	0.017
L-Alanine	2TMS	223.1267	5.97	1,053	9,963 ± 1,767/36,233 ± 13,799	0.27	0.100
	3TMS	305.1663	8.76	1,279	5,900 ± 335/96,467 ± 20,766	0.06	0.017
Phosphate	3TMS	314.0959	7.85	1,236	53,233 ± 28,407/170,000 ± 17,578	0.31	0.003
L-Proline	2TMS	259.1424	8.15	1,250	5,400 ± 1,542/63,433 ± 7,250	0.09	0.003
Succinic acid	2TMS	262.1057	8.32	1,258	49,300 ± 4,078/81,567 ± 15,815	0.60	0.048
Fumaric acid	2TMS	260.0900	8.68	1,275	3,907 ± 457/7,900 ± 123	0.49	0.006
Malic acid	2TMS	350.1401	9.96	1,441	3,880 ± 98/17,833 ± 981	0.22	0.001
Glucose[f]	5TMS, 1MeOx[g]	569.2876	13.44	1,852	433,667 ± 12,423/3,757 ± 45	115.44	0.0003
Maltose[h]	8TMS, 1MeOx	947.459	16.38	2,659	3,553 ± 983/127 ± 27	28.05	0.027
Trehalose[i]	8TMS	918.4324	18.49	2,661	433,333 ± 26,312/476,000 ± 17,349	0.91	0.158

[a] RT, retention time during gas chromatography.
[b] RI, retention index calculated using alkane standards (C_{10} to C_{40}).
[c] Integrated area of chromatographic peak under P_i-limiting conditions versus P_i-excess conditions. Values are means and standard deviations from triplicate experiments.
[d] Determined by Student's *t* test.
[e] TMS, trimethylsilyl.
[f] Glucose levels are relatively uncertain due to possible contamination by glucose of the medium during the extraction process; P_i-limited cells retain high glucose concentrations in the medium after 24 h of cultivation.
[g] MeOX, methoxyamine.
[h] Maltose was detected only by the EI mode due to its higher molecular mass and was extracted with cold methanol.
[i] Trehalose data were included despite a *P* value of >0.05, as trehalose can serve as a precursor for maltose by the action of trehalose synthase (TreS).

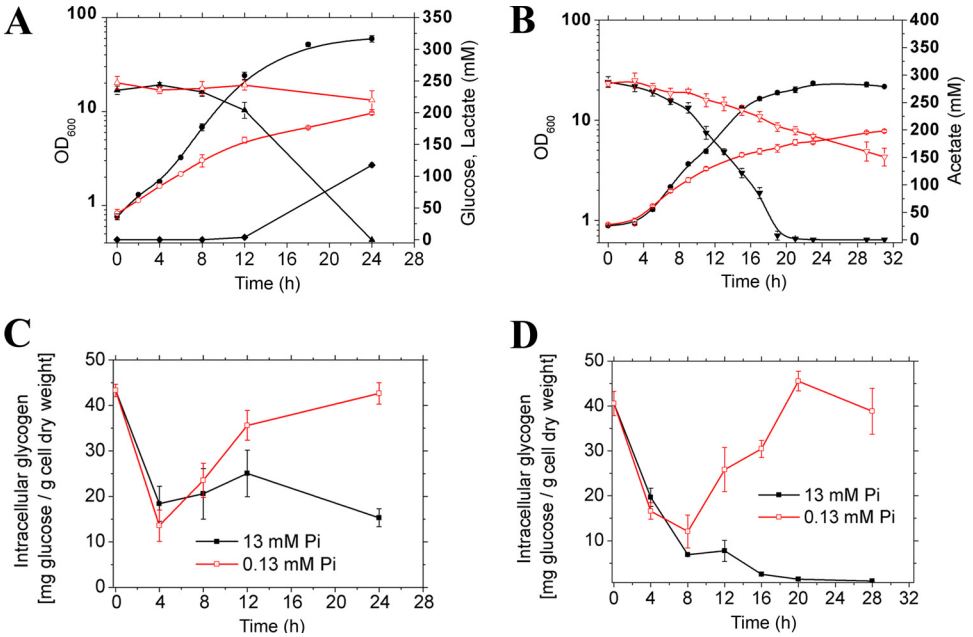

FIG. 2. Growth (OD_{600}, circles), carbon source consumption (triangles), and cellular glycogen pools (squares) are shown for *C. glutamicum* cultivated in CGXII minimal medium with 222 mM glucose (A and C) or with 300 mM potassium acetate (B and D) either under P_i excess or P_i limitation. The inoculum was precultivated twice in the same medium under P_i limitation. Panel A also shows lactate formation (rhombic symbols), which did not occur during growth on acetate (B). Mean values and standard deviations of triplicate cultures are shown.

The detection of glycolic acid in *C. glutamicum* extracts was unexpected, as this compound has not been described yet as a metabolite in this organism and no pathway leading to glycolate in *C. glutamicum* is known. L-Alanine was detected in two forms, as a 2-fold trimethylsilyl-modified form and a 3-fold trimethylsilyl-modified form. Both forms showed a reduced level in the P_i-limited cells. As L-alanine is derived from pyruvate, this result might be a consequence of a reduced glycolytic flux and a reduced pyruvate pool during P_i limitation. Also, three intermediates of the tricarboxylic acid (TCA) cycle showed reduced levels in P_i-limited cells, namely, succinate, malate, and fumarate. L-Proline, which is formed from L-glutamate, showed a greatly reduced pool under P_i limitation, which could be due to a reduced TCA cycle flux and reduced levels of NADPH or ATP.

The metabolites that showed the most greatly increased levels in P_i-limited cells were glucose (115-fold) and maltose (28-fold). Whereas the ratio measured for glucose might be caused by contamination through the high concentration of external glucose that was still present in the medium of the P_i-limited cultures after 24 h, the increased pool of maltose cannot be explained in this way. As outlined below, it is related to glycogen metabolism.

Phosphorus-containing-metabolite profiling of *C. glutamicum* using ^{31}P-NMR spectroscopy. To complement GC-MS analysis, *in vivo* ^{31}P-NMR was applied to measure different intracellular phosphorus-containing metabolites in *C. glutamicum* cells cultivated under either P_i excess or limitation. The results are summarized in Fig. 3. The cytoplasmic P_i concentration after 24 h of growth was calculated to be 17.5 ± 0.72 mM under P_i excess and 1.8 ± 0.01 mM under P_i limitation. This difference (9.7-fold) is larger than the one determined by GC-MS (3-fold) but reflects the native situation accurately. The concentration of phosphomonoesters was also found to be much lower in P_i-starved cells (4.0 ± 0.16 mM after 24 h) than in P_i-excess cells (27.1 ± 1.4 mM after 24 h). Similarly, the concentration of NDP-glucose was about 6-fold lower in P_i-starved cells (0.16 ± 0.13 mM after 24 h) than P_i-excess cells (1.07 ± 0.28 mM after 24 h). Polyphosphate was detected in stationary-phase cells grown under P_i excess but not in cells grown under P_i limitation, as expected.

Influence of the transcriptional regulator SugR on the glucose uptake rate under P_i limitation. The DeoR-type transcriptional regulator SugR represses genes of the phosphoenolpyruvate phosphotransferase system (PTS), genes of several glycolytic enzymes, and a variety of further metabolic genes (8, 9, 11, 40–42). The repressing function of SugR has been reported to be relieved by several sugar phosphates, i.e., fructose 6-phosphate, fructose 1-phosphate, glucose 6-phosphate, and fructose 1,6-bisphosphate (9, 11, 42). The levels of these metabolites are high when cells grow on sugars, such as glucose or fructose, and low when the cells grow on gluconeogenic carbon sources, such as acetate. As the level of P_i monoesters in glucose-grown cells was found to be much lower in P_i-starved cells, the question of whether the low glucose uptake rates observed for cells growing under P_i limitation [46 nmol min^{-1} (mg of protein)$^{-1}$ compared to 192 nmol min^{-1} (mg of protein)$^{-1}$ under P_i excess] might be related to the activity of SugR arose.

To test this possibility, we analyzed growth and glucose consumption of a Δ*sugR* mutant of *C. glutamicum* (9) under P_i excess and P_i starvation. As shown in Fig. 4, the Δ*sugR* mutant grew similarly to the wild type under P_i limitation, but to a lower optical density. Under P_i excess, on the other hand, the

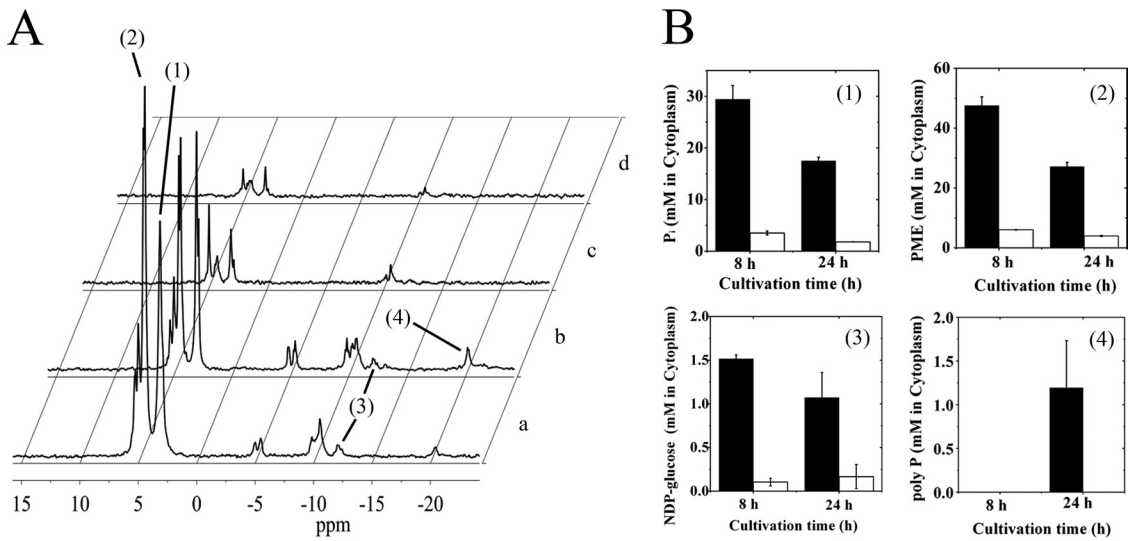

FIG. 3. *In vivo* ^{31}P-NMR spectrum (A) and measurements to determine the cytoplasmic concentrations of intracellular P_i, phosphate monoesters (PME), NDP-glucose, and polyphosphate (polyP) in cells cultivated for 8 h (a) and 24 h (b) in CGXII glucose minimal medium with 13 mM P_i (black bars) or for 8 h (c) and 24 h (d) in CGXII glucose minimal medium with 0.13 mM P_i (white bars) (B). Signals representing intracellular P_i (1), phosphate monoesters (2), NDP-glucose (3), and polyphosphate (4) are marked in the ^{31}P-NMR spectra, which were recorded using a Varian Inova 400 MHz spectrometer operating at a ^{31}P frequency of 161.985 MHz, as described in Materials and Methods. The experiment was performed twice with comparable results.

Δ*sugR* mutant reached a higher optical density than the wild type. Under P_i excess, the glucose consumption rate of the Δ*sugR* mutant was comparable to that of the wild type, whereas it was 2.5-fold higher (114 nmol min^{-1} [mg of protein]$^{-1}$) under P_i limitation (the period from 8 h to 24 h after start of the cultivation was used for calculation). This supports the assumption that the low glucose consumption rate under P_i limitation is at least partially due to repression of the PTS genes for glucose uptake (*ptsG*, *ptsI*, and *ptsH*) and of glycolytic genes by SugR, due to low levels of its effector metabolites. The major reason for the low glucose consumption rate under P_i limitation might, however, be a low rate of phosphoenolpyruvate (PEP) formation.

Influence of P_i limitation on the glycogen pool of *C. glutamicum*. *C. glutamicum* cells growing on glucose, fructose, or sucrose accumulate glycogen up to 90 mg per g of cells (dry weight) in the early exponential growth phase and degrade the polymer when the sugar becomes limiting. In contrast, only marginal amounts of glycogen are formed in cells growing on the gluconeogenic substrates acetate or lactate (36). Recent studies revealed a close connection between maltose and glycogen metabolism (38). The finding of a greatly increased maltose pool in P_i-limited cells prompted us to also measure the glycogen content of cells. As shown in Fig. 2, there was a significant discrepancy between results obtained under P_i-limiting and P_i-excess conditions. Comparable to previously published data (36), cells grown on glucose under P_i excess accumulated glycogen up to 30 mg glucose per g of cells (dry weight) in the early exponential growth phase and then started to degrade it before reaching the stationary phase. In contrast, P_i-limited cells accumulated glycogen up to 24 h to a level of about 45 mg glucose per g of cells (dry weight). Even more surprising was the observation that cells grown with acetate as the sole carbon source also formed glycogen under P_i limitation up to levels comparable to that of glucose-grown cells (Fig. 2C and D). In agreement with previous results (36), no glycogen was formed by acetate-grown cells under P_i excess (Fig. 2D). The high glycogen level that was measured at time zero in all cultures resulted from the precultivation of the inoculum under P_i-limiting conditions. Based on these results, P_i limitation causes glycogen accumulation in *C. glutamicum*.

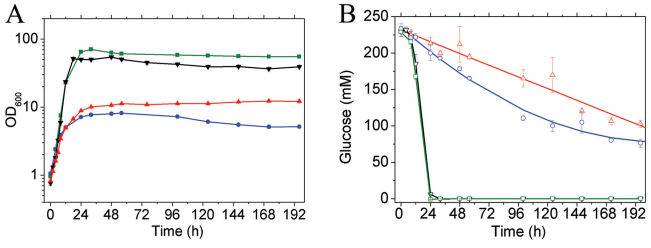

FIG. 4. Growth of (A) and glucose consumption by (B) of *C. glutamicum* wild type (black and red) and the Δ*sugR* mutant (green and blue) in CGXII minimal medium with 4% (wt/vol) glucose and either 13 mM P_i (black and green) or 0.13 mM P_i (red and blue). Mean values and standard deviations of triplicate cultures are shown.

The results described above raised the question of whether also other types of growth limitations have an influence on glycogen accumulation. Therefore, the glycogen content was measured in *C. glutamicum* cells cultivated either under nitrogen excess and nitrogen limitation or under iron excess and iron limitation. Both types of stresses have been studied in the past, and key players involved in the adaptation to these stresses have been identified (for reviews, see references 4 and 10). As shown in Fig. S4 in the supplemental material, these limitations did not cause an accumulation of glycogen in the stationary phase during growth on glucose or acetate. This

TABLE 3. Influence of P_i concentration on the expression of the *pgm* and *glgC* genes in *C. glutamicum*

Growth condition	CAT activity[a] (nmol min^{-1} mg $protein^{-1}$)	
	C. glutamicum pET2-*pgm*	*C. glutamicum* pET2-*glgC*
P_i excess (13 mM)	31 ± 5	195 ± 37
P_i limitation (0.13 mM)	189 ± 37	583 ± 6

[a] Strains were cultivated for 24 h in CGXII medium with 222 mM glucose under either P_i excess or P_i limitation. Chloramphenicol acetyltransferase activities were determined using cell-free extracts. Means and standard deviations derived from three independent cultivations are given.

indicates that glycogen accumulation is one of the specific responses of the cell to P_i limitation.

Influence of P_i limitation on the expression of *pgm* and *glgC*. Glycogen synthesis in *C. glutamicum* involves four enzymes, i.e., phosphoglucomutase (*pgm*), catalyzing the conversion of glucose 6-phosphate to glucose 1-phosphate, ADP-glucose pyrophosphorylase (*glgC*), which converts glucose 1-phosphate and ATP to ADP-glucose and pyrophosphate, glycogen synthase (*glgA*), converting $[\alpha\text{-1,4-glucan}]_n$ and ADP-glucose to $[\alpha\text{-1,4-glucan}]_{n+1}$ and ADP, and branching enzyme (*glgB*), which introduces α-1,6-glycosidic bonds into linear α-1,4-glucans. To test the influence of P_i limitation on the expression of *pgm* and *glgC*, the corresponding promoter regions were cloned into the promoter probe vector pET2 containing a promoterless chloramphenicol acetyltransferase reporter gene, and the resulting plasmids pET2-*pgm* and pET2-*glgC* were transferred into *C. glutamicum* wild type. As shown in Table 3, expression of the phosphoglucomutase gene *pgm* was 6-fold higher in cells grown for 24 h under P_i limitation than in cells grown for 24 h under P_i excess. In the case of the ADP-glucose pyrophosphorylase gene *glgC* the expression level was 3-fold higher under P_i limitation than P_i excess. These results indicate that genes of the glycogen synthesis pathway are activated or derepressed under P_i limitation, and increased levels of the two enzyme activities could be at least partially responsible for the increased flux of glucose 6-phosphate into the glycogen pathway and reduced fluxes into glycolysis and the pentose phosphate pathway.

***In silico* simulation of the phosphate starvation response using a genome-scale model of *C. glutamicum*.** In order to study the influence of P_i limitation on metabolism *in silico* by flux balance analysis (FBA), a genome-scale model of *C. glutamicum* (20) was expanded by including two reactions required for glycogen synthesis (ADP-glucose pyrophosphorylase and glycogen synthase) and one reaction responsible for glycogen degradation, which represents both glycogen phosphorylase and maltodextrin phosphorylase. The resulting optimal phenotypes for growth under variation of glucose and P_i uptake are shown in Fig. 5A. As expected, under the precondition of a sufficient glucose uptake rate (>4 mmol [g of cells (dry weight)]$^{-1}$ h^{-1}), the growth rate is linearly dependent on the P_i uptake rate. However, there is a discrepancy between the simulated maximal growth rate and the experimentally determined growth rate under P_i-limiting conditions, the latter being located at a point where no steady-state flux solution of the network exists. To reach the experimentally observed growth rate of about 0.16 h^{-1} under P_i limitation in the simulation, glucose and phosphate uptake rates have to be significantly higher (>2 mmol g of cells (dry weight)$^{-1}$ h^{-1} and >0.1 mmol g of cells (dry weight)$^{-1}$ h^{-1}, respectively). A similar observation was made for the results obtained for the acetate-grown cells. Here discrepancies were found for both phosphate-limiting and phosphate-excess conditions (Fig. 5B). As expected, simulations showed that increasing the glucose or acetate uptake rate at low phosphate uptake rates would not lead to higher cellular growth.

Since a strong influence of P_i limitation on the glycogen pool was observed (see above), the influence of varying glucose and phosphate uptake rates on glycogen formation was tested *in silico*. As shown in Fig. 5C, an increased rate of glycogen synthesis was predicted at low P_i uptake and high glucose uptake rates. The same behavior was also observed when acetate instead of glucose was used as carbon source (Fig. 5D). These predictions are in agreement with the experimental results.

DISCUSSION

Previous studies on the response of bacteria to P_i-limiting conditions focused mainly on gene expression, regulators, and enzymes involved in the P_i starvation response. In the work presented here, the influence of P_i limitation on metabolite levels was analyzed by GC-MS using *C. glutamicum* as a model organism. An important result was the detection of greatly elevated maltose levels under P_i limitation, which raises the question of how this disaccharide is formed in cells growing on glucose. The only pathway that has been described in literature for *C. glutamicum* is the conversion of trehalose to maltose by trehalose synthase (TreS). TreS was shown to be the only enzyme present in *C. glutamicum* capable of converting trehalose to maltose and *vice versa*, and evidence that TreS is mainly responsible for trehalose degradation was presented (48). Trehalose, which serves as a stress protection compound and as a prerequisite for mycolate production, is synthesized either from UDP-glucose and glucose 6-phosphate via the OtsA-OtsB pathway or from malto-oligosaccharides or α-1,4-glucans via the TreY-TreZ pathway (43, 48). The cytoplasmic trehalose level as determined by GC-MS was much higher than the maltose level (by a factor of 10^3 to 10^4) and was only slightly decreased under P_i-limitation compared to P_i-excess.

Besides TreS, one alternative enzyme candidate could also play a role in maltose formation. The protein encoded by *cg1012* shows sequence similarity to the *E. coli* maltodextrin glucosidase MalZ. MalZ removes glucose residues from the reducing end of maltodextrins, which are composed of more than two glucose residues (i.e., maltotriose, maltotetraose, etc.), and forms maltose as an end product (5). It is not yet clear whether this enzyme activity is present in *C. glutamicum* (38), but it would offer an alternative explanation for the high internal glucose level of P_i-limited cells (besides the possibility that it is due to contamination from residual extracellular glucose).

Recent studies have indicated that *C. glutamicum* catabolizes maltose in the same way as *E. coli* (2) by MalQ (*cg2523*), a maltodextrin glucanotransferase (also called amylomaltase) which forms from any maltodextrin, including maltose, larger

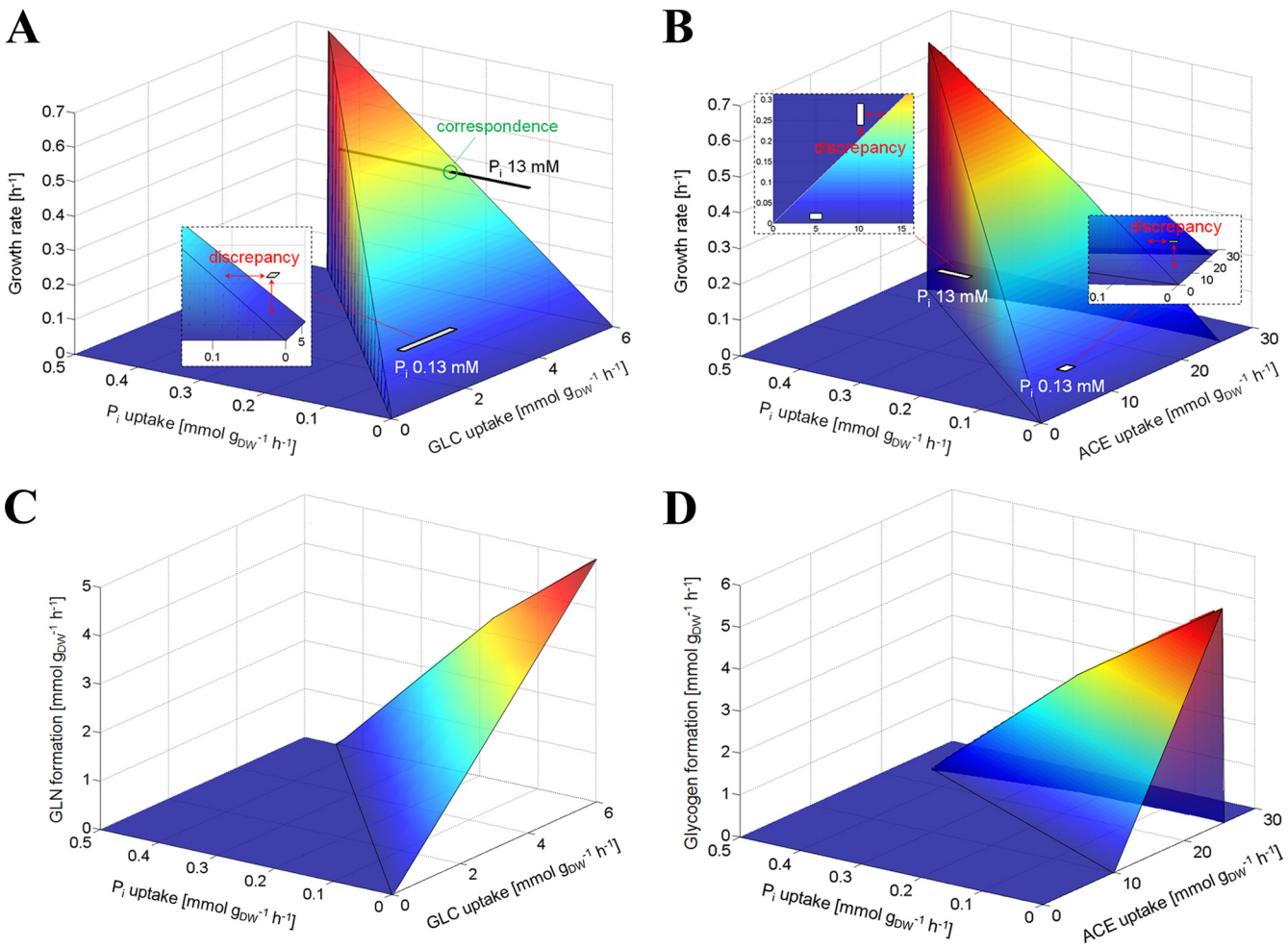

FIG. 5. Simulated phenotypes under growth optimization of the genome-scale metabolic network model. *In silico* solutions of growth rates and glycogen (GLN) formation under variation of P_i uptake in combination with either glucose (GLC) uptake (A and C) or acetate (ACE) uptake (B and D) form three-dimensional surfaces in each case. For comparison, measured growth rates for P_i-limited and -excess cultures, including experimental errors, are mapped as light gray rectangles.

maltodextrins, and glucose. Glucose can then be phosphorylated either by an ATP-dependent glucokinase (30) or by a polyphosphate/NTP-dependent glucokinase (25) to glucose 6-phosphate and catabolized, whereas the maltodextrins are degraded by maltodextrin phosphorylase (MalP) to glucose 1-phosphate, which is converted to glucose 6-phosphate by phosphoglucomutase (38). In *Mycobacterium tuberculosis* and *M. smegmatis*, maltose formed from trehalose by TreS is incorporated into glycogen by the consecutive action of the maltose kinase Pep1 and the maltosyltransferase GlgE (7, 17). Genes encoding homologs of Pep1 (*cg2530*) and GlgE (*cg1382*) were also identified in *C. glutamicum* but have not yet been characterized (G. M. Seibold, unpublished data).

In a previous study, the presence of maltose in cells of *C. glutamicum* cultivated on glucose under P_i excess was reported (39). Thus, maltose might be a regular metabolite in *C. glutamicum* not only during growth on maltose. The question of whether the increased maltose pool observed under P_i-limitation is caused by an increased synthesis or by a decreased degradation or both cannot be answered at the moment.

Based on the close connection of maltose and glycogen metabolism, we found that P_i starvation also had a strong influence on the cellular glycogen pool. Whereas under P_i excess, glycogen is formed in the early exponential phase and then degraded again, P_i-starved cells form a glycogen pool in the exponential phase but also retain it in the stationary phase, irrespective of whether glucose or acetate was used as the carbon source. The large glycogen pool under P_i starvation could be due to increased synthesis, as suggested by the increased expression of *pgm* and *glgC*. The regulators responsible for this increased expression are not yet known. The global transcriptional regulator RamA was recently shown to function as an activator of *glgC* (37), but current knowledge suggests that RamA responds to a metabolite involved in acetate catabolism rather than to P_i. Besides an increased glycogen synthesis rate, a decreased glycogen degradation rate could also be responsible for the altered glycogen pool under P_i limitation. Glycogen degradation in *C. glutamicum* involves glycogen phosphorylase (GlgP), which phosphorolytically cleaves α-1,4-glycosidic bonds at the nonreducing ends of glycogen and

forms glucose 1-phosphate and phosphorylase-limited dextrins. The debranching enzyme (GlgX) converts these dextrins to linear maltodextrins ($2 < n < 20$, where n is the number of glucose molecules), which are then further degraded by MalP to glucose 1-phosphate (38). As GlgP and MalP both require P_i, their activity might be limited at reduced cytoplasmic P_i concentrations.

The *in silico* simulation data based on a stoichiometric genome-scale metabolic model (20) that was modified to include glycogen synthesis and degradation reactions predicted increased glycogen formation in exponentially growing cells under P_i limitation with glucose or acetate as the carbon source. However, the model was not able to correctly predict the experimentally determined growth rates under P_i starvation. Reasons for the observed discrepancies could be a lack of qualitative information and/or quantitative accuracy of the model, which mainly includes all biomass-related reactions but only rough estimations of its stoichiometric coefficients. Furthermore, the model does not incorporate any kind of P_i-dependent regulation of central metabolism and storage pool metabolism (glycogen, polyphosphate). An inclusion of regulation would necessitate the formulation of mechanistic models, which is currently impossible due to the lack of quantitative knowledge of regulatory and metabolic processes. Therefore, the results from our stoichiometric analysis should be regarded as a first step in simulating the complex metabolism of carbohydrate storage pools like glycogen.

Central carbon metabolism and energy metabolism are inevitably connected to the availability of P_i, as key enzymatic reactions require P_i as substrate, such as glyceraldehyde 3-phosphate dehydrogenase and F_1F_o-ATP synthase. In addition, many reactions require ATP or ADP as substrates, such as phosphofructokinase, 3-phosphoglycerate kinase, and pyruvate kinase. As the cytoplasmic concentrations of P_i, ADP, and ATP are lower under P_i-limiting conditions, a reduced enzyme activity and consequently a reduced glycolytic flux can be envisaged, resulting in a reduced PEP synthesis rate and thus a reduced glucose consumption rate. In this study, another consequence of P_i limitation was found, namely, an altered glycogen metabolism resulting in an increased and more stable glycogen pool. To our knowledge, such a link has not yet been described. Further studies are required to elucidate the molecular details of this connection.

ACKNOWLEDGMENTS

This work was financially supported by the German Ministry of Education and Research (BMBF) within the program "GenoMikPlus" (grant 0313805D to M.B.).

We thank Volker Wendisch and Verena Engels for providing the *C. glutamicum* Δ*sugR* strain and Katharina Nöh for valuable contributions at the beginning of this project.

REFERENCES

1. **Becker, S. A., A. M. Feist, M. L. Mo, G. Hannum, B. O. Palsson, and M. J. Herrgard.** 2007. Quantitative prediction of cellular metabolism with constraint-based models: the COBRA toolbox. Nat. Protocols **2:**727–738.
2. **Boos, W., and H. Shuman.** 1998. Maltose/maltodextrin system of *Escherichia coli*: transport, metabolism, and regulation. Microbiol. Mol. Biol. Rev. **62:** 204–229.
3. **Burkovski, A. (ed.).** 2008. Corynebacteria: genomics and molecular biology. Caister Academic Press, Norfolk, United Kingdom.
4. **Burkovski, A.** 2007. Nitrogen control in *Corynebacterium glutamicum*: proteins, mechanisms, signals. J. Microbiol. Biotechnol. **17:**187–194.
5. **Dippel, R., and W. Boos.** 2005. The maltodextrin system of *Escherichia coli*: metabolism and transport. J. Bacteriol. **187:**8322–8331.
6. **Eggeling, L., and M. Bott (ed.).** 2005. Handbook of *Corynebacterium glutamicum.* CRC Press, Taylor & Francis Group, Boca Raton, Florida.
7. **Elbein, A. D., I. Pastuszak, A. J. Tackett, T. Wilson, and Y. T. Pan.** 2010. Last step in the conversion of trehalose to glycogen: a mycobacterial enzyme that transfers maltose from maltose 1-phosphate to glycogen. J. Biol. Chem. **285:**9803–9812.
8. **Engels, V., S. N. Lindner, and V. F. Wendisch.** 2008. The global repressor SugR controls expression of genes of glycolysis and of the L-lactate dehydrogenase LdhA in *Corynebacterium glutamicum*. J. Bacteriol. **190:**8033–8044.
9. **Engels, V., and V. F. Wendisch.** 2007. The DeoR-type regulator SugR represses expression of *ptsG* in *Corynebacterium glutamicum*. J. Bacteriol. **189:** 2955–2966.
10. **Frunzke, J., and M. Bott.** 2008. Regulation of iron homeostasis in *Corynebacterium glutamicum*, p. 241–266. *In* A. Burkovski (ed.), Corynebacteria: genomics and molecular biology. Caister Academic Press, Norfolk, United Kingdom.
11. **Gaigalat, L., J. P. Schlüter, M. Hartmann, S. Mormann, A. Tauch, A. Pühler, and J. Kalinowski.** 2007. The DeoR-type transcriptional regulator SugR acts as a repressor for genes encoding the phosphoenolpyruvate: phosphotransferase system (PTS) in *Corynebacterium glutamicum*. BMC Mol. Biol. **8:**104.
12. **Hermann, T.** 2003. Industrial production of amino acids by coryneform bacteria. J. Biotechnol. **104:**155–172.
13. **Hsieh, Y. J., and B. L. Wanner.** 2010. Global regulation by the seven-component Pi signaling system. Curr. Opin. Microbiol. **13:**198–203.
14. **Hulett, F. M.** 2002. The Pho regulon, p. 193–201. *In* J. A. Sonenshein and R. M. Losick (ed.), *Bacillus subtilis* and its closest relatives: from genes to cells. ASM Press, Washington, DC.
15. **Ishige, T., M. Krause, M. Bott, V. F. Wendisch, and H. Sahm.** 2003. The phosphate starvation stimulon of *Corynebacterium glutamicum* determined by DNA microarray analyses. J. Bacteriol. **185:**4519–4529.
16. **Kabus, A., A. Niebisch, and M. Bott.** 2007. Role of cytochrome *bd* oxidase from *Corynebacterium glutamicum* in growth and lysine production. Appl. Environ. Microbiol. **73:**861–868.
17. **Kalscheuer, R., K. Syson, U. Veeraraghavan, B. Weinrick, K. E. Biermann, Z. Liu, J. C. Sacchettini, G. Besra, S. Bornemann, and W. R. Jacobs.** 2010. Self-poisoning of *Mycobacterium tuberculosis* by targeting GlgE in an α-glucan pathway. Nat. Chem. Biol. **6:**376–384.
18. **Keilhauer, C., L. Eggeling, and H. Sahm.** 1993. Isoleucine synthesis in *Corynebacterium glutamicum*: molecular analysis of the *ilvB-ilvN-ilvC* operon. J. Bacteriol. **175:**5595–5603.
19. **Kinoshita, S., S. Udaka, and M. Shimono.** 1957. Studies on amino acid fermentation. Part I. Production of L-glutamic acid by various microorganisms. J. Gen. Appl. Microbiol. **3:**193–205.
20. **Kjeldsen, K. R., and J. Nielsen.** 2009. *In silico* genome-scale reconstruction and validation of the *Corynebacterium glutamicum* metabolic network. Biotechnol. Bioeng. **102:**583–597.
21. **Kocan, M., S. Schaffer, T. Ishige, U. Sorger-Herrmann, V. F. Wendisch, and M. Bott.** 2006. Two-component systems of *Corynebacterium glutamicum*: deletion analysis and involvement of the PhoS-PhoR system in the phosphate starvation response. J. Bacteriol. **188:**724–732.
22. **Lambert, C., D. Weuster-Botz, R. Weichenhain, E. W. Kreutz, A. A. De Graaf, and S. M. Schoberth.** 2002. Monitoring of inorganic polyphosphate dynamics in *Corynebacterium glutamicum* using a novel oxygen sparger for real time P-31 *in vivo* NMR. Acta Biotechnol. **22:**245–260.
23. **Lee, S. H., H. M. Woo, B. H. Jung, J. G. Lee, O. S. Kwon, H. S. Pyo, M. H. Choi, and B. C. Chung.** 2007. Metabolomic approach to evaluate the toxicological effects of nonylphenol with rat urine. Anal. Chem. **79:**6102–6110.
24. **Liebl, W.** 2005. *Corynebacterium* taxonomy, p. 9–34. *In* L. Eggeling and M. Bott (ed.), Handbook of *Corynebacterium glutamicum*. CRC Press, Taylor & Francis Group, Boca Raton, FL.
25. **Lindner, S. N., S. Knebel, S. R. Pallerla, S. M. Schoberth, and V. F. Wendisch.** 2010. Cg2091 encodes a polyphosphate/ATP-dependent glucokinase of *Corynebacterium glutamicum.* Appl. Microbiol. Biotechnol. doi:10.1007/s00253-010-2568-5.
26. **Lindner, S. N., S. Knebel, H. Wesseling, S. M. Schoberth, and V. F. Wendisch.** 2009. Exopolyphosphatases Ppx1 and Ppx2 from *Corynebacterium glutamicum*. Appl. Environ. Microbiol. **75:**3161–3170.
27. **Lindner, S. N., H. Niederholtmeyer, K. Schmitz, S. M. Schoberth, and V. F. Wendisch.** 2010. Polyphosphate/ATP-dependent NAD kinase of *Corynebacterium glutamicum*: biochemical properties and impact of *ppnK* overexpression on lysine production. Appl. Microbiol. Biotechnol. doi:10.1007/s00253-010-2481-y.
28. **Lindner, S. N., D. Vidaurre, S. Willbold, S. M. Schoberth, and V. F. Wendisch.** 2007. NCgl2620 encodes a class II polyphosphate kinase in *Corynebacterium glutamicum*. Appl. Environ. Microbiol. **73:**5026–5033.
29. **Pallerla, S. R., S. Knebel, T. Polen, P. Klauth, J. Hollender, V. F. Wendisch, and S. M. Schoberth.** 2005. Formation of volutin granules in *Corynebacterium glutamicum*. FEMS Microbiol. Lett. **243:**133–140.

30. **Park, S. Y., H. K. Kim, S. K. Yoo, T. K. Oh, and J. K. Lee.** 2000. Characterization of *glk*, a gene coding for glucose kinase of *Corynebacterium glutamicum*. FEMS Microbiol. Lett. **188:**209–215.
31. **Parrou, J. L., and J. Francois.** 1997. A simplified procedure for a rapid and reliable assay of both glycogen and trehalose in whole yeast cells. Anal. Biochem. **248:**186–188.
32. **Price, N. D., J. L. Reed, and B. O. Palsson.** 2004. Genome-scale models of microbial cells: evaluating the consequences of constraints. Nature Rev. Microbiol. **2:**886–897.
33. **Rittmann, D., U. Sorger-Hermann, and V. F. Wendisch.** 2005. Phosphate starvation-inducible gene *ushA* encodes a 5′ nucleotidase required for growth of *Corynebacterium glutamicum* on nucleotides as the phosphorus source. Appl. Environ. Microbiol. **71:**4339–4344.
34. **Schaaf, S., and M. Bott.** 2007. Target genes and DNA-binding sites of the response regulator PhoR from *Corynebacterium glutamicum*. J. Bacteriol. **189:**5002–5011.
35. **Seibold, G., M. Auchter, S. Berens, J. Kalinowski, and B. J. Eikmanns.** 2006. Utilization of soluble starch by a recombinant *Corynebacterium glutamicum* strain: growth and lysine production. J. Biotechnol. **124:**381–391.
36. **Seibold, G., S. Dempf, J. Schreiner, and B. J. Eikmanns.** 2007. Glycogen formation in *Corynebacterium glutamicum* and role of ADP-glucose pyrophosphorylase. Microbiology **153:**1275–1285.
37. **Seibold, G. M., C. T. Hagmann, M. Schietzel, D. Emer, M. Auchter, J. Schreiner, and B. J. Eikmanns.** 2010. The transcriptional regulators RamA and RamB are involved in the regulation of glycogen synthesis in *Corynebacterium glutamicum*. Microbiology **156:**1256–1263.
38. **Seibold, G. M., M. Wurst, and B. J. Eikmanns.** 2009. Roles of maltodextrin and glycogen phosphorylases in maltose utilization and glycogen metabolism in *Corynebacterium glutamicum*. Microbiology **155:**347–358.
39. **Strelkov, S., M. von Elstermann, and D. Schomburg.** 2004. Comprehensive analysis of metabolites in *Corynebacterium glutamicum* by gas chromatography/mass spectrometry. Biol. Chem. **385:**853–861.
40. **Tanaka, Y., H. Teramoto, M. Inui, and H. Yukawa.** 2008. Regulation of expression of general components of the phosphoenolpyruvate: carbohydrate phosphotransferase system (PTS) by the global regulator SugR in *Corynebacterium glutamicum*. Appl. Microbiol. Biotechnol. **78:**309–318.
41. **Toyoda, K., H. Teramoto, M. Inui, and H. Yukawa.** 2008. Expression of the *gapA* gene encoding glyceraldehyde 3-phosphate dehydrogenase of *Corynebacterium glutamicum* is regulated by the global regulator SugR. Appl. Microbiol. Biotechnol. **81:**291–301.
42. **Toyoda, K., H. Teramoto, M. Inui, and H. Yukawa.** 2009. Molecular mechanism of SugR-mediated sugar-dependent expression of the *ldhA* gene encoding L-lactate dehydrogenase in *Corynebacterium glutamicum*. Appl. Microbiol. Biotechnol. **83:**315–327.
43. **Tzvetkov, M., C. Klopprogge, O. Zelder, and W. Liebl.** 2003. Genetic dissection of trehalose biosynthesis in *Corynebacterium glutamicum*: inactivation of trehalose production leads to impaired growth and an altered cell wall lipid composition. Microbiology **149:**1659–1673.
44. **Vasicova, P., Z. Abrhamova, J. Nesvera, M. Patek, H. Sahm, and B. Eikmanns.** 1998. Integrative and autonomously replicating vectors for analysis of promoters in *Corynebacterium glutamicum*. Biotechnol. Techniques **12:** 743–746.
45. **Wanner, B. L.** 1996. Phosphorus assimilation and control of the phosphate regulon, p. 1357–1381. *In* F. C. Neidhardt et al. (ed.), *Escherichia coli* and *Salmonella*: cellular and molecular biology, 2nd ed., vol. 1. ASM Press, Washington, DC.
46. **Wendisch, V. F., and M. Bott.** 2005. Phosphorus metabolism, p. 377–396. *In* L. Eggeling and M. Bott (ed.), Handbook of *Corynebacterium glutamicum*. CRC Press, Boca Raton, FL.
47. **Wold, S., M. Sjöström, and L. Eriksson.** 2001. PLS-regression: a basic tool of chemometrics. Chemom. Intell. Lab. Syst. **58:**109–130.
48. **Wolf, A., R. Krämer, and S. Morbach.** 2003. Three pathways for trehalose metabolism in *Corynebacterium glutamicum* ATCC13032 and their significance in response to osmotic stress. Mol. Microbiol. **49:**1119–1134.